TS-based RSM-aided design of cold-formed steel stiffened C-sectional columns susceptible to buckling

P. Deniziak & K. Winkelmann

Gdansk University of Technology, Faculty of Civil and Environmental Engineering, Gdansk, Poland

ABSTRACT: The paper focuses on joint-performance analysis of a built-up cold-formed thin-walled C-sectional column with a fillister (stiffener) of the same type, interconnected with a series of bolts located along the length of the compressed members in specific spacing. The quantity of bolts and the non-connected starting distance of the fillister are considered random variables of the problem. Optimal distribution of joints on the stiffener is found by means of Response Surface Methodology, based on Targeted Sampling technique. The critical load of the column is the response of the random model, dependent on random input parameters. The load values are computed by means of discrete realizations of the column FE model.

1 INTRODUCTION

Cold-formed thin-walled steel elements have been widely used since the EN 1993-1-3 appearance. Their relatively low weight and shaping ease makes them very popular. The promotion of thin-walled elements may decrease investments cost up to 25% and reach the limit steel reserve up to 50%, as indicated in Brodka et al. 2007.

Many companies have patented their individual cross-sectional shapes, more complicated shapes are designed nowadays, see Lukowicz et al 2016.

A unique cross-sectional shape, proposed by Llentab Group is analysed in the paper. The experimental results of such cold-formed sections are presented in Gordziej-Zagorowska et al. 2016 and Urbanska-Galewska et al. 2016.

2 GEOMETRY DETAILS OF THE COLUMN

The compressed column analysed in this paper consists of two cold-formed, thin-walled C-sections (outer: 360x100x43x3mm, inner: 300x75x43x3mm), interconnected by rows of four M12 self-drilling bolts with a reduced drill point per each row. The thickness of cold-formed steel sheets is 3 mm.

The closely spaced inner C-section is not situated along the whole length of the element, it acts only as a reinforcing stiffener in the central part of the column, leaving the top and bottom unreinforced. The total height of the column is equal to 3500mm.

The cross-section of the column is shown in Figure 1, whereas a full layout is given in Figure 2.
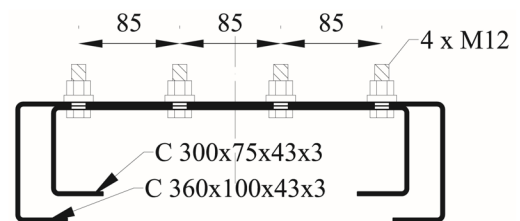

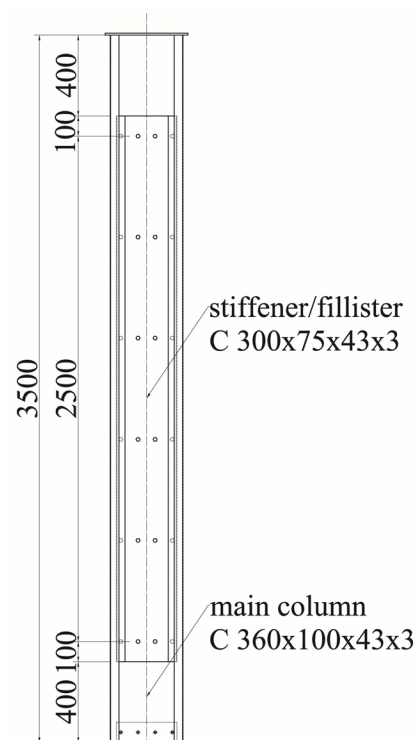Figure 1. Cross-section of the analyzed compressed column.

Figure 2. Side view of the analyzed compressed column.

3 FE MODEL OF THE COLUMN

The FEM analysis was carried out in Dlubal RFEM v.5.07 commercial software.

The column was made of S350GD steel, with material constants equal to $E = 210$ GPa and $v = 0.30$. An isotropic non-linearly elastic material was assumed, no additional strain hardening modulus was introduced. The total dead weight of the column is equal to 0.87 kN.

The column main chords were modelled by means of 58 shell elements spanned on 216 nodes, the connectors (bolts) were assumed a joint of two round surfaces (shell elements without membrane tension) with a round bar between the shells of a diameter of 12 mm, with the number of bars dependent on the undertaken model (8-32 elements). It is worth noting, that no contact elements or laws were assumed between the C-sections. This approach is common in the axial symmetry of eigenmodes of a compressed stiffener.

The structure was supported to achieve a double hinged beam boundary conditions. The bottom line support is shown in Figure 3.

The S4R shell elements were used, their meshing is set to 10 mm for C-sections webs and 20 mm for flanges. The vicinity of bolts is also provided with additional mesh refinements.

The second-order analysis (P-Delta/P-delta) was performed, with a chosen PICARD solution method. In every step of the analysis five load increments were generated to reach a reliable limit load value.

The column was subjected to an axially compressive linear load, situated on the top edge. The load action is shown in Figure 3.

The main goal of the analysis was to determine the critical load value of the column (N_{cr}) corresponding to the occurrence of buckling. At first the operation was performed for the starting geometry of the column, next it was computed for a set of design variants of the bolts quantity/location. While considering an initial column geometry, the load was equal to 150.2 kN.
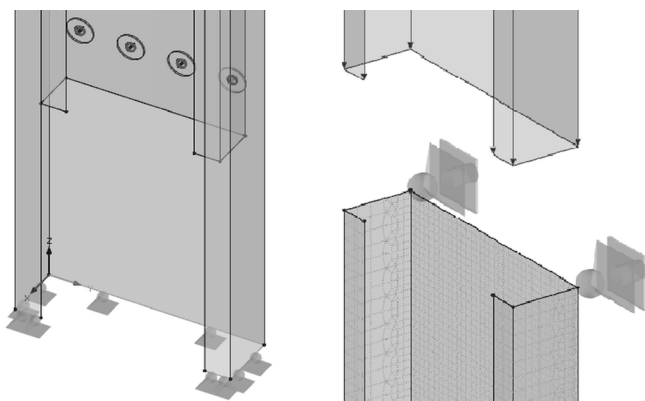

Figure 3. FE model visualizations of support region (left) and load region (right), provided by Dlubal RFEM software.

4 TARGETED SAMPLING (TS) APPROACH

4.1 *Adopted random parameters*

Two random parameters were taken for the task – the quantity of the bolts and the non-connected starting distance of the fillister. Both were assumed discrete random variables, the boundary values of their distributions were set to represent the extreme possible design dimensions of the column. The probabilities of their singletons were equal to $(1/n_{sin})$, n_{sin} is the amount of singletons.

The non-connected starting distance of the fillister was denoted by d [mm] and taken as the first random variable, x_1. Its set of singletons consists of 11 values, spaced linearly from $d_{min} = 100$ mm to $d_{max} = 1100$ mm every 100 mm. Note, that Figure 2 shows the parameter d equal to 100 mm.

The quantity of bolts, equal to a number of their possible rows n [-] was taken as the second random variable, x_2. The second set of singletons consist of 7 values only, spaced linearly from $n_{min} = 2$ rows (giving 8 bolts in total) to $n_{max} = 8$ rows (32 bolts in total). Figure 2 shows the parameter n is equal to 6.

4.2 *Analyzed targeted samples*

According to the TS technique, four key groups of samples were generated from the most significant pairs of singletons. The first group contained only the middle point sample ($d_m = 600$ mm, $n_m = 5$ rows) and it was taken as the starting point of the analysis. The following group was made of four corner ($d_c;n_c$) samples: (100;2), (100;8), (1100;2) and (1100;8). The next group of six samples was taken from the sensitivity analysis, matching one random parameter set at its mean value and making the second parameter variable with a set step. Because the parameters vary in terms of singleton quantity, only two samples: (600;3), (600;7) were generated along the x_2 dimension, while four samples: (100;5), (300;5), (900;5), (1100;5) were generated along the x_1. It should be noted, that the middle point sample was taken away from the set, so the doubling of its numerical weight was omitted. The last set consisted of four diagonal samples, generated with a proportional change in both parameters: (300;3), (300;7), (900;3), (900,7). The middle point sample, as well as the corner samples, were not included in the group.

4.3 *Numerical computing of the TS samples*

A number of 15 samples are generated using the TS approach, out of possible number of 77 (7×11).

The pairs of the parameters are imposed on the numerical model, and the corresponding critical load of the column (N_{cr}) is calculated for every sample, resulting in a coupled structural response value $g(x_1,x_2)$ of each sample.

The numerical model generated on the basis of the exemplary corner sample (1100;8) result is shown in Figure 4. Although it was generated unshapely in terms of structural design, its importance in the TS technique is proved crucial in the further analysis.
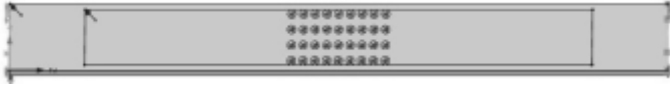

Figure 4. A visualization (horizontal) of a numerical model generated using an exemplary corner sample ($d = 1100$; $n = 8$).

5 RESPONSE SURFACE METHODOLOGY

On the basis of the performed model realizations, the response surface of the phenomena is computed, using two approximation models – the first order equation, given by Eq. (1) and the second order approximation with cross-terms, given by Eq. (2).

$$\bar{y}(\mathbf{x}) = \beta_0 + \sum_{i=1}^{n} \beta_i x_i = \beta_0 + \beta_1 x_1 + \beta_2 x_2 \quad (1)$$

$$\bar{y}(\mathbf{x}) = \beta_0 + \sum_{i=1}^{n} \beta_i x_i + \sum_{i=1}^{n} \beta_{ii} x_i^2 + \sum_{i<j}^{n} \sum_{j=2}^{n} \beta_{ij} x_i x_j$$
$$= \beta_0 + \beta_1 x_1 + \beta_2 x_2 + \beta_{11} x_1^2 + \beta_{22} x_2^2 + \beta_{12} x_1 x_2 \quad (2)$$

The analysis is carried out in steps well-suited for tests of these types. At first, the points are taken in a center-to-edge approach: Series 1 consisted of 7 points (central × 1 + sensitivity × 6), Series 2 – of 11 points (previous + diagonal × 4) and Series 3 – of all 15 points. Secondly, the points are taken in an edge-to-center approach: Series 1* consisted of 5 points (central × 1 + corner × 4), Series 2* – of 9 points (previous + diagonal × 4). The series 3 was mutual for both approaches. For a 2nd-order approximation, the latter approach is the only way to obtain convergent results, see Winkelmann & Gorski 2014.

For the comparison purposes, approximation was done of an adequate order, incorporating all 77 structural response values from every singleton available in the task, as a reference solution.

The solutions were assessed by means of an adequate error estimator, given by Eq. (3):

$$\varepsilon_{\bar{y}(\mathbf{x})} = \frac{100\%}{3} \cdot \sum_{i=1}^{3} \left| 1 - \frac{\beta_{calc}}{\beta_{exact}} \right| \; or \; \frac{100\%}{6} \cdot \sum_{i=1}^{6} \left| 1 - \frac{\beta_{calc}}{\beta_{exact}} \right| \quad (3)$$

where $\beta = \{\beta_0; \beta_1; \beta_2; \beta_{11}; \beta_{22}; \beta_{12}\}$ are the following six slope factors (approximated), β_{calc} denotes the calculated value of a respective slope factor in each series of the analysis, whereas β_{exact} is the value taken from an second-order approximation of the structural response using all 77 samples.

All the key response surfaces of the considered phenomenon were approximated using a proprietary, dedicated software RSM-Win, see Winkelmann et al. 2017.

All results were also further checked in terms of a graphical analysis (SciLab software), which is a basic standard in the analysis of structural response surface, see Winkelmann 2014.

6 RESULTS

6.1 First-order RS approximation

Five sets of numerical nodes of the surface – both Series 1-3 and Series 1*-2* were considered in the first-order approximation. The results of the calculations are presented in Table 1.

The high-quality results of the 1st-order approximation (both the reference solution and the Series 3 15-sample approximation) are shown in Figures 5-6.

Table 1. Approximation results of the first-order model – the projected response surface equations.

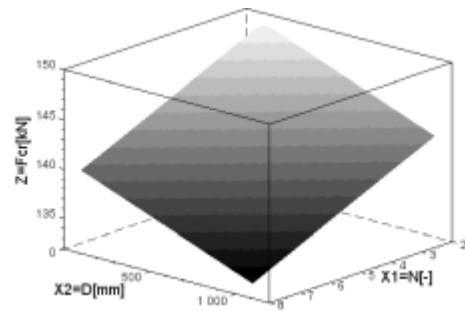| Series	RS equation	Error
Reference (77)	$152.610 - 1.284 \cdot x_1 - 0.006833 \cdot x_2$	N/A
Series 3 (15)	$153.141 - 1.260 \cdot x_1 - 0.007436 \cdot x_2$	3.45%
Series 2 (11)	$154.280 - 1.350 \cdot x_1 - 0.008625 \cdot x_2$	8.92%
Series 1 (7)	$155.729 - 1.450 \cdot x_1 - 0.010632 \cdot x_2$	16.39%
Series 2* (9)	$151.794 - 1.245 \cdot x_1 - 0.006297 \cdot x_2$	4.06%
Series 1* (5)	$151.680 - 1.200 \cdot x_1 - 0.006200 \cdot x_2$	5.94%

Figure 5. 1st order RS approximation – the reference solution.
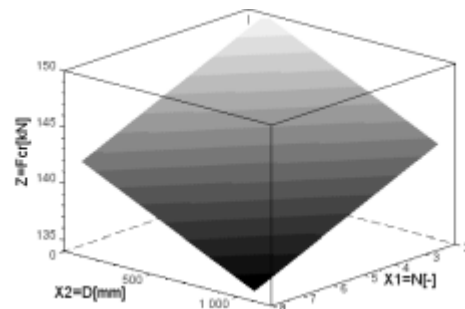

Figure 6. 1st order RS approximation – 15 samples (Series 3).

It should be pointed out, that a 15-sample approximation is satisfactory here, leading the error to 3.5%. Hence 20% of a total number of possible samples result in a similar quality, which results in 1/5 of the computational cost of a full solution.

The edge-to-center approach was proved desirable, the comparable center-to-edge approach brought an exponentially bigger estimation error.

While adopting only the central + corner samples in the calculations, the approximation error slightly exceeded 5%, so the result was trustworthy and sufficient. This means, that for such a simple structural model, five samples taken in accordance to TS technique recommendations led to an accurate structural response pattern despite computing only ca 6.5% of column's possible geometry variants.

6.2 *Second-order RS approximation*

Three sets of numerical nodes of the surface (Series 1*, 2* and 3) were considered in the 2nd-order approximation. The results are presented in Table 2.

The 2nd-order approximation result in the case of 15 samples is shown in Figure 7.

The 2nd-order approximation based on 15 samples is better than the linear one, the error was lower than 2.5%. However, the quadratic slope factors influence the total error – a lower number of samples makes the computational quality decrease, and the discrepancy to the reference solution unallowable.

Table 2. Approximation results of the second-order model – the projected response surface equations.

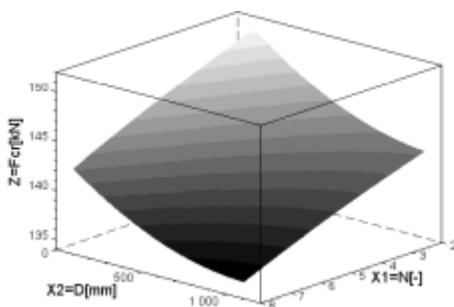| Series	RS equation	Error
Reference (77)	$152.610-1.044 \cdot x_1-0.014847 \cdot x_2 -0.3424 \cdot 10^{-1} \cdot x_1^2+0.6425 \cdot 10^{-5} \cdot x_2^2 +0.1549 \cdot 10^{-3} \cdot x_1 \cdot x_2$	N/A
Series 3 (15)	$154.343-1.024 \cdot x_1-0.015854 \cdot x_2 -0.3289 \cdot 10^{-1} \cdot x_1^2+0.6368 \cdot 10^{-5} \cdot x_2^2 +0.1551 \cdot 10^{-3} \cdot x_1 \cdot x_2$	2.53%
Series 2* (9)	$157.192-1.423 \cdot x_1-0.023962 \cdot x_2 -0.2884 \cdot 10^{-1} \cdot x_1^2+0.3945 \cdot 10^{-5} \cdot x_2^2 +0.1667 \cdot 10^{-3} \cdot x_1 \cdot x_2$	26.04%
Series 1* (5)	$159.6327-1.383 \cdot x_1-0.027211 \cdot x_2 -0.2401 \cdot 10^{-1} \cdot x_1^2+1.1221 \cdot 10^{-5} \cdot x_2^2 +0.1667 \cdot 10^{-3} \cdot x_1 \cdot x_2$	91.70%

Figure 7. 2nd-order RS approximation – 15 samples (Series 3).

7 CONCLUSIONS

It has been proved that a TS-based RSM-aided analysis is helpful in the design process of simple structural elements, the selected case was a stiffened cold-formed thin-walled steel C-sectional column.

The undertaken method provides a basic outline for the design in about 1/15 of the time required for an exact response computation.

Based on the computed structural response surface the complexity of the problem is also highlighted – in this case a simple and swift 1st-order analysis was sufficient for the undertaken task.

The 2nd-order approximation is recommended only when taking a large sample space into account. Moreover, the samples should be distributed sparsely, otherwise the algorithm was divergent, see also Biegus 1999, Winkelmann 2014.

The peak value of the phenomenon is reached for a simulation marked by $d = 100$ mm, $n = 2$ rows. This indicated either the importance of weakening of the column web due to the holes for joints or the impossibility to neglect the contact between the main column and the fillister. The topic will be subjected to further experimental analysis by the Authors.

REFERENCES

Biegus, A. 1999. Probabilistic analysis of steel structures (*in polish*). PWN, Warsaw.

Brodka, J., Broniewicz, M & Gizejowski, M. 2007. Cold-formed sections – designer's guide (*in polish*). PWT, Warsaw.

Lukowicz, M., Deniziak, P., Migda, W., Gordziej-Zagorowska, M. & Szczepanski, M. 2016. Innovative cold-formed GEB section under compression. *Recent Progress in Steel and Composite Structures*: 107-114.

Gordziej-Zagorowska, M., Urbanska-Galewska, E., Pyrzowski, L. Deniziak, P. & Lukowicz, M. 2016. Preliminary experimental research on stability of truss' joint with positive eccentricity. *Recent Progress in Steel and Composite Structures*: 425–432.

Urbanska-Galewska, E., Deniziak, P., Gordziej-Zagorowska, M., & Lukowicz, M. 2016. Thin-walled cross section shape influence on steel members resistance. *Advances in Science and Technology Research Journal*: 41–45.

Winkelmann, K. 2014 The use of response surface methodology for reliability estimation of aluminum silo subjected to wind load. *Shell Structures: Theory and Applications. Vol. 3*: 571-574.

Winkelmann, K. & Górski, J. 2014. The use of response surface methodology for reliability estimation of composite engineering structures. *Journal of Theoretical and Applied Mechanics* 52(4): 1019–1032.

Winkelmann, K., Jakubowska, P. & Soltysik, B. 2017. Reliability assessment of an OVH HV power line truss transmission tower subjected to seismic loading. *Scientific Session of Applied Mechanics IX. AIP Conference Proceedings* 1822: 020016.